



## Original Paper

# Statistical assessment of the financial performance of shale-gas wells coupling stochastic and numerical simulation



Andres Soage <sup>a, b, \*</sup>, Luis Ramirez <sup>a</sup>, Ruben Juanes <sup>c, d</sup>, Luis Cueto-Felgueroso <sup>b</sup>, Ignasi Colominas <sup>a</sup>

<sup>a</sup> Group of Numerical Methods in Engineering-GMNI, Center for Technological, Innovation in Construction and Civil Engineering-CITEEC. Civil Engineering School, University of a Coruña, Campus of Elviña, A Coruña, 15008, Galicia, Spain

<sup>b</sup> Department of Civil Engineering: Hydraulics, Energy and Environment. Polytechnic University of Madrid, Madrid, 28006, Spain

<sup>c</sup> Department of Civil and Environmental Engineering, Massachusetts Institute of Technology, Cambridge, 02139, MA, USA

<sup>d</sup> Department of Earth, Atmospheric and Planetary Sciences, Massachusetts Institute of Technology, Cambridge, 02139, MA, USA

## ARTICLE INFO

## Article history:

Received 16 May 2023

Received in revised form

15 July 2024

Accepted 17 July 2024

Available online 20 July 2024

Edited by Jia-Jia Fei and Min Li

## Keywords:

Gas volatility

Shale gas

Net present value

Internal rate return

Stochastic model

Financial estimator

Monte Carlo simulation

Kernel density function

## ABSTRACT

We present a new methodology to statistically determine the net present value (NPV) and internal rate of return (IRR) as financial estimators of shale gas investments. Our method allows us to forecast, in a fully probabilistic setting, financial performance risk and to understand the importance of the different factors that impact investment. The methodology developed in this study combines, through Monte Carlo simulation, the computational modeling of gas production from shale gas wells with a stochastic simulation of gas price as a geometric Brownian motion (GMB). To illustrate the methodology's validity, we apply it to an analysis of investments in shale gas wells. Our results show that gas price volatility is a key variable in the performance of an investment of this type, in such a way that at high volatilities, the potential return on an investment in shale gas increases significantly, but so do the risks of economic loss. This finding is consistent with the history of shale gas operations in which huge investment successes coexist with unexpected investment failures.

© 2024 The Authors. Publishing services by Elsevier B.V. on behalf of KeAi Communications Co. Ltd. This is an open access article under the CC BY-NC-ND license (<http://creativecommons.org/licenses/by-nc-nd/4.0/>).

## 1. Introduction

Shale gas wells are facilities that allow the extraction of light hydrocarbons trapped in ultra-impermeable formations (Curtis, 2002). These types of wells have led to a boom in the oil and gas (O&G) industry, completely transforming the energy landscape (Wang et al., 2014). The development of shale gas wells has relied on the refinement of two technologies: directional drilling and hydraulic fracturing.

Directional drilling allows wells to be drilled at great depths (1500 to 3000 m) and along great horizontal lengths (1000 to 5000 m). Hydraulic fracturing refers to the injection of water mixed with other compounds at high pressures, which fractures the shale-type formation, creating a network of fractures that allows the

release of the trapped gas (Osborn et al., 2011).

Shale gas operations involve very large financial investments, which require thorough financial studies to make adequate investment decisions.

Making rational financial decisions requires having tools that rank investments based on their potential profitability and risk level (Barro, 2015; Dittmar and Yuan, 2008; Haley and Schall, 1973; Levy and Sarnat, 1978; Mentel and Horváthová, 2016).

For investments made in movable assets such as bonds, analysts use static methodologies to calculate the value of financial estimators (e.g., return of equity, ROE) and compare investments (Poggensee and Poggensee, 2021). These are called static methods due to the fact that the variation in the investment over time is not taken into consideration. More specifically, investments are studied assuming that financial aspects such as revenues, costs or amortizations are constant throughout their life (Damodaran, 2008; Mangiero and Michael, 2017). Other types of financial analysis tools

\* Corresponding author.

E-mail address: [a.soage@udc.es](mailto:a.soage@udc.es) (A. Soage).

are based on dynamic methodologies that take into account the evolution of an investment over time (Perez, 2014). This type of approach to financial indicators improves decision-making, giving more precise information to the analyst (Melcher and Melcher, 1980; Hacura et al., 2001). Investments made in non-movable capital (e.g., real estate assets) are usually analyzed using dynamic methods. The most commonly used investment estimators for these types of investments are the net present value (NPV) and the internal rate of return (IRR) (Bhandari, 1985; Dorfman, 1981; Gallo, 2014; León, 2012; Ross, 1995).

In this study, we propose a methodology for the development of dynamic financial analysis tools for shale gas investments that include an estimate of the probability of the occurrence or financial risks or their quantification. We numerically generate probability density functions (PDFs) of the financial estimators NPV and IRR. The numerical procedure that we use combines numerical calculations of the production of natural gas from shale gas wells with stochastic processes of the natural gas market price as a geometric Brownian motion (GBM). Through Monte Carlo simulation, we calculate different values of NPV and IRR, to which we numerically fit a PDF of Gaussian kernels using the numerical kernel density estimation (KDE) method. Finally, we analyze the goodness of fit using the Kolmogorov–Smirnov test (K-S test) (Massey, 1951; Sheather and Jones, 1991).

According to (Energy Information Administration, 2016), in the USA, the costs of onshore O&G wells range from 4.9 to 8.3 million US dollars, whereas the costs of deep offshore wells range from 120 to 230 million US dollars per well. Investments of such magnitude require evaluation tools that enable appropriate decision making. The NPV and IRR are the financial estimators most commonly used to analyze the viability of investments in the O&G industry, in particular shale gas wells (Bas, 2013; Eshkalak et al., 2014; Hong et al., 2020; Lake et al., 2013; Nguyen-Le and Shin, 2019; Soage et al., 2021; Weijermars, 2013; Yu and Sepehrnoori, 2013).

Financial risk quantification is essential when calculating the NPV or IRR for making long-term and high-cost investments (Ranasinghe and Russell, 2006). We address this issue in the shale gas industry by considering the sources of uncertainty. These sources of uncertainty in shale gas wells can be categorized into two main types:

- Uncertainty from processes of a financial nature: This category includes the uncertainty of the gas price's evolution throughout the project and the evolution of inflation.
- The uncertainty in gas production throughout the well's lifetime: An uncertainty which has two simultaneous sources:
  - Uncertainty of the shale gas well's petrophysical properties, such as its porosity.
  - Uncertainty in the actual outcome of the well's design parameters, such as the geometry of the stimulated fractured volume.

In this work, we address the inherent uncertainty of gas price variation considering the price evolution of this asset as a process which follows a GBM (Cano and Andrés, 2010; Gimeno, 2018; Lindén, 2018). We base the selection of this calculation method on the assumption of the efficient market hypothesis (EMH) in its weak form (Fama, 1970; Malkiel, 2013; Stein, 1989). According to the EMH, all market players act rationally, and the valuation of an asset instantly considers all information pertaining to the asset. The weak version of this hypothesis assumes the existence of certain randomness in the valuation of an asset, due to the existence of unexpected news that can affect the price of an asset. When applying the weak EMH, econometric methods are no longer valid

when predicting the gas price. We must use stochastic methods for forecasting the gas price value. Stochastic methods are combined with Monte Carlo simulation to obtain multiple gas price trajectories (Hacura et al., 2001; Papadopoulos and Yeung, 2001; Ye and Tiong, 2000).

We forecast gas production using calculations of the numerical model of shale gas wells described previously (Soage, 2021; Soage et al., 2021). In this paper, the authors implement numerical simulations with parametric sweeping of the variables considered most important in the economic performance of shale gas.

We estimate the cash flow of the basic shale gas well described previously (Soage et al., 2021) by combining gas production simulations for different parameters with stochastic gas price simulations. We consider all the economic data (e.g., CAPEX, inflation, or taxes) to calculate the NPV and IRR distributions for each parameter and all price simulations.

We obtain the distribution of NPV or IRR values, applying a PDF to the outputs of both financial estimators. We also calculate the cumulative density function (CDF) and determine the 10%, 50%, and 90% percentiles. We determine the valuation of these investments with a certain risk or probability of occurrence. This quantitative assessment enables shale gas investors to be aware of different NPV or IRR values for the well, along with the associated probability of this value occurring (Armeanu and Lache, 2009; Johar et al., 2010).

Several methodologies have already been proposed for the study of financial investments in shale gas. A general block of studies analyze NPV and IRR as financial indicators taking constant or quasi-constant values of costs and incomes. Income is determined by the price of gas and the total gas production from the wells. The costs are associated with the initial investment made (CAPEX) and the costs of time-dependent operations (OPEX). Additionally, the costs of taxation, currency depreciation, and the amortization of the investment can be incorporated into the expenses, and government implementation subsidies can even be considered as a cost reduction. This approach has proven to be very useful, especially in macro-scale financial studies at the level of basins or regions (Chen et al., 2015; Cooper et al., 2018; Liu et al., 2020; Nguyen-Le and Shin, 2019).

Another set of studies seeks to incorporate uncertainty in the study of financial feasibility (i.e., “uncertainty approximations”). Some of these studies assume that the price of gas is known since it is regulated or is considered constant as hypothesis. In these studies, gas production, petrological parameters, or fracture systems are subject to high uncertainty, and it is thus necessary to model them using stochastic approaches (Bai et al., 2013; Li et al., 2018; Naraghi and Javadpour, 2015; Rammay and Awotunde, 2016; Wu et al., 2021). There are other studies within the field of “uncertainty approximations” that focus on the random and stochastic nature of the gas price and well execution costs. They are based on the use of Monte Carlo simulation and its variants, applying it to the characterization of these financial indicators (Chebeir et al., 2017; Drouven et al., 2017; Kaiser, 2012; Liu et al., 2022; Yuan et al., 2015).

Our approach would fit into the class of studies with uncertainty but with a new angle, combining the random nature of both the gas price and methane production in shale-type formations. We performed parametric scans of the porosity and kerogen amount (petrological variables). We also conducted parametric sweeps of fracture permeability in the stimulated shale volume and the geometry of the fractured volumes (geomechanical variables). These sweeps were carried out via numerical simulation, and from them we obtain different gas production curves. For its part, we carry out gas price simulations considering different drift and volatility values. All of this information is grouped together in the determination of sets of values of the financial estimators and their

adjustment to a probability function.

The aim of this article is to seek an almost purely probabilistic approach that deals with the uncertainty of both price and production. With this objective, we obtain the value of the NPV and the IRR of an investment in shale gas in a probabilistic and non-deterministic way and using a novel methodology.

In this study, we do not consider the uncertainty of cost, and we perform parametric combinations of production considering the rest of the constant parameters. In future studies, and as an additional step in this work, total statistical variability of the set of relevant aspects in the financial performance of investments in shale gas could be included.

## 2. Materials and methods

### 2.1. Introduction

In this first subsection, we give an overview of the methodology that we follow in this study.

First, we develop a 3D numerical model of a standard-design shale gas well.

Next, using this numerical model, we perform calculations of methane production curves over an exploitation period of 10 years. These curves are calculated for different values of porosity, amounts of kerogen, induced permeabilities in the stimulated volume, and geometries of the effectively fractured and propped ellipsoids.

In addition to these gas production considerations, we analyze the historical price of gas. We study it under the hypothesis that the price trajectories respond to a geometric Brownian motion. Using Monte Carlo simulation, we generate thousands of synthetic gas price series over a 10-year time period. We vary the drift and volatility of the stochastic process and generate four different price scenarios.

Finally, we combine the gas price series with the gas production series. Thus, we obtain a probability density function of the financial indicators NPV and IRR.

### 2.2. Numerical simulation of shale gas production

In this subsection, we briefly describe the numerical model of shale gas production that was extensively explained in a prior study (Soage et al., 2021, 2024). This numerical model is based on other previous studies (Kazmouz et al., 2016; Patzek et al., 2013; Silin and Kneafsey, 2012; Yao et al., 2013).

In this study, we carry out the analysis of shale gas production through numerical simulation. We consider a shale gas well with standard characteristics. The well is located at a depth of 3000 m in the middle layer of a 90-m-thick shale stratum. The lateral length of the well is 1500 m, and it has 7 hydraulic fractures executed every 200 m. Each of the hydraulic fractures produces a highly stimulated ellipsoidal zone with high permeability. These ellipsoidal zones have axes with the following dimensions: 300 × 40 × 70 m. The mathematical formulations that describe gas production in a well with these characteristics are as follows:

$$\alpha \frac{\partial P}{\partial t} + \left[ \nabla \cdot \left( \frac{c_g \cdot k}{\mu} \right) P(\nabla P) \right] = 0, \quad (1)$$

$$\alpha = (c_g \phi + \rho_0 \rho_k S_k c_f), \quad (2)$$

$$P(\mathbf{x}, 0) = P_r \text{ in } \Omega, P(\mathbf{x}, t) = P_{\text{bhp}} \text{ in } \Gamma, \quad (3)$$

$$V_a = \frac{V_L P}{P_L + P}, \quad (4)$$

$$q(t) = \iint_{\Gamma} \left( \frac{-2c_g k}{\mu} P \right) \nabla P \cdot \bar{\mathbf{n}} d\Gamma. \quad (5)$$

A schematic representation of the shale gas well described in this section appears in Fig. 1. In Table 1, we list all the variables appearing in Eqs. (1)–(5), along with their definition and parameter values.

This mathematical model allows us to calculate the evolution of the pressure field. During the variation of the pressure field, we calculate the flow of methane gas.

To solve Eqs. (1)–(5), we used the COMSOL Multiphysics 6.1 simulator (COMSOL Multiphysics, 2018). We carried out the simulation with the finite element method in a volume of stimulated shale rock. This volume is called the stimulated recovery volume (SRV). In this case, it has a prismatic shape and dimensions of 1800 × 600 × 90 m. We generated a mesh of tetrahedral elements within the SRV. We consider that the horizontal section of the well is an internal domain boundary along most of its length. To ensure an accurate numerical solution, we generated a finer mesh in the EPVs. The outer boundaries of the SRV are considered to be no-flow boundaries. We consider that the initial pressure in the reservoir is 30 MPa, and once hydraulic fracturing occurs, an imposed pressure of 5 MPa is reached at the intersection of the centroid of the EPVs with the well. These points correspond to the well perforations for fracturing the rock. These perforations are also the areas through which methane flows into the well. The evolution of pressure and gas production was analyzed over 10 years of simulation. Fig. 1 includes an illustration of the 3D mesh to carry out the simulations of this study.

It is worth highlighting the most relevant petrological aspects of this study. The porosity of the shale-type formation is assumed to be 3%, with an initial permeability of 1 nanodarcy (1 nD), equivalent to 10<sup>-21</sup> m<sup>2</sup>. After hydraulic stimulation, the SRV reaches a permeability of 0.01 millidarcy (0.01 md), which can be expressed as 10<sup>-17</sup> m<sup>2</sup>. The volumes of the EPVs, having been subjected to a very high fluid pressure, reach a permeability of 2 md ≈ 2 × 10<sup>-15</sup> m<sup>2</sup>. The porosity and permeability values are assumed to be constant over time, homogeneous and isotropic throughout the study domain (Kazemi and Takbiri-Borujeni, 2015; Song et al., 2016; Zhang et al., 2019; Zhao et al., 2018; Zhou et al., 2021). The amount of kerogen is assumed to be 10%. This distribution is considered to remain constant throughout the entire shale formation. The adsorption of methane to kerogen is described by the Langmuir isotherm (Cristancho-Albarracin et al., 2017; Psarras et al., 2017; Wang et al., 2017; Yu et al., 2016). Furthermore, we consider that the volume of highly fractured rock due to the effect of the fluid injected at high pressure has an ellipsoidal geometry. For the same type of injected fluid and a given pressure, it is the tensional state of the shale rock and its geomechanical properties that determine the degree of flatness or sphericity of the EPVs. We consider that these rock properties have a constant distribution in the volume of the SRV (Nassir et al., 2017; Wei et al., 2016; Zhang et al., 2017).

In this study, we carried out a parametric scan of the petrological values (porosity and amount of kerogen), as well as the parameters that mark the efficiency of hydraulic fracturing (induced permeability and flatness of the EPVs). The two parameters related to fracturing efficiency are closely linked to the geomechanical parameters of the formation. A parametric sweep was performed by varying one parameter of every four study parameters while maintaining the initial value of the other three. The total number of

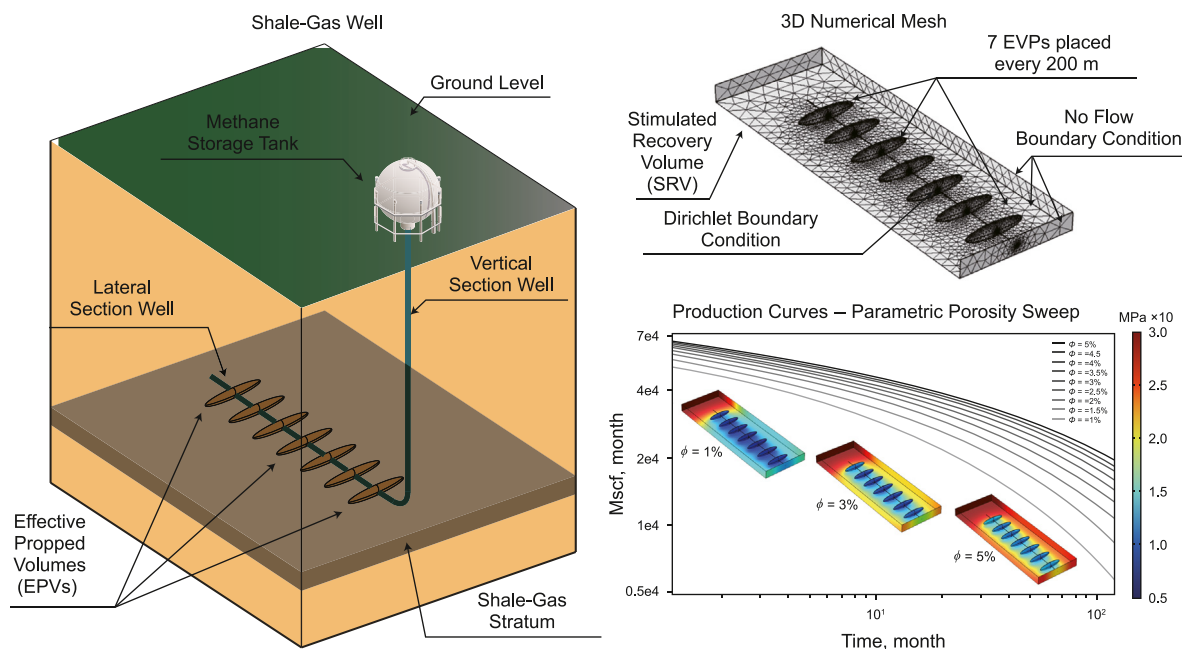


**Fig. 1.** Representation of the shale gas well used in this article. Three-dimensional finite element mesh used to carry out the simulations. Results of production curves and pressure states of the SRV after 10 years of simulated sweeping of different porosity values.

**Table 1**  
Variables and parameters.

Variable	Meaning	Value
$P(\mathbf{x}, t)$	Gas pressure, MPa	30–5
$P_i$	Initial reservoir pressure, MPa	30
$P_{bhp}$	Bottom hole pressure, MPa	5
$C_g$	Gas compressibility, $s^2/m^2$	$3.979 \times 10^{-6}$
$c_f$	Langmuir isotherm slope, $m^4 \times s^2/kg^2$	–
$\phi$	Porosity	1%–5%
$\rho_0$	Methane density at standard conditions, $kg/m^3$	0.717
$\rho_k$	Kerogen density, $kg/m^3$	1250
$S_k$	Kerogen relative volume	10%
$V_a$	Langmuir isotherm, $m^3/kg$	–
$V_L$	Langmuir volume, $m^3/kg$	0.00264
$P_L$	Langmuir pressure, MPa	3
$k$	Fractured shale permeability, $m^2$	$10^{-18}$ – $10^{-17}$ ( $\approx 1$ – $10 \mu D$ )
$k_{EPV}$	EPV permeability, $m^2$	$2 \times 10^{-15}$ , ( $\approx 2 mD$ )
$\mu$	Methane viscosity, $10^{-4} Pa \cdot s$	–
$q$	Methane flux, Mscf/month <sup>a</sup>	–
$\Omega$	Stimulated volume	–
$\bar{n}$	Normal vector to contour $\Gamma$	–

<sup>a</sup> Mscf/month ( $1 m^3 \sim 0.0353$  Mscf).

variations of the four parameters across all their values generates an extremely high calculation time cost that it is not possible to address in this study. The porosity was varied between 1% and 5% by performing gas production calculations every 0.5 porosity points. We varied the permeability of the SRV between  $10^{-18}$  and  $10^{-17} m^2$ , with an increase in permeability of  $1.9 \times 10^{-18} m^2$  in each production study. The amount of kerogen was scanned between 1% and 15%, with an increment of 2% for each production curve. Finally, to analyze the impact of the flatness of the EPVs on gas production, we carried out 17 studies. We started with a length of the semi-axis of the EPVs contained in the plane of the well and perpendicular to it of 235 m and a semi-axis contained in the plane of the well and longitudinal to it of 12.77 m. In each study of the scan, the major axis was reduced by 15 m and the minor axis increased in a corresponding proportion to keep the volume of the EPVs constant. In this way, we went from flat EPVs perpendicular to the well to a

spherical shape and, finally, to EPVs that are longitudinal to the well and intersect each other. We assume as a hypothesis that as long as the volume of highly fractured rock (EPVs) remains constant, the cost of hydraulic fracturing will also remain constant.

### 2.3. Geometric brownian motion (GBM) applied to gas price forecasting

Firstly, we study the characteristics of the natural gas price time series. For simplicity, we refer to natural gas and methane, CH<sub>4</sub>, interchangeably.

We take the Henry Hub Spot Price (HHSP) as a reference for the natural gas price. The Henry Hub is a gas pipeline hub located in Erath, Louisiana (USA), property of the company Sabine Pipe Line LLC. Due to the importance of this gas pipeline hub, the spot price of this natural gas asset and its futures listed on the New York

Mercantile Exchange are given the same name. The price is defined in USD per millions of British Thermal Units (USD/MMBTU), and its value strongly correlates with all other prices, regulated or unregulated, of natural gas on other markets or at other positions in the network, such as at the head well (Lake et al., 2013).

The U.S. Energy Information Administration (EIA) website provides HHSP data at different frequencies (daily, weekly, monthly, or yearly) from the 6th of January 1997 to the 16th of April 2020. We show these data at a daily frequency in Fig. 2, which also includes the most relevant statistical data of this time series.

Modeling gas prices as a geometric Brownian motion (GBM), the governing equation over time is as follows:

$$P_t = P_0 \cdot e^{\left[ \left( \mu - \frac{1}{2} \sigma^2 \right) \sigma t + \sigma \xi_t \sqrt{t} \right]} \tag{6}$$

In Eq. (6), a reference price value  $P_0$  is used to calculate the gas price,  $P_t$ , at time  $t$ . The parameter  $\mu$  is the drift or trend of the process,  $\sigma$  is the volatility of the asset, and  $\xi_t$  is a white-noise-type random process with distribution  $\xi_t \sim N(0,1)$ .

We use Eqs. (7) and (8) to estimate the drift and volatility based on the gas price historical data:

$$\hat{\mu} = \frac{1}{N \cdot \Delta t} \sum_{i=1}^N \left( \frac{P_i}{P_{i-1}} - 1 \right), \tag{7}$$

$$\hat{\sigma}^2 = \frac{1}{N \cdot \Delta t} \sum_{i=1}^N \left( \frac{P_i}{P_{i-1}} - 1 - \hat{\mu} \Delta t \right)^2. \tag{8}$$

In these equations,  $P_i$  is the price of gas at instant  $i$ ,  $P_{i-1}$  is the price of gas at instant  $i-1$ ,  $\Delta t$  is the time step between two natural gas price observations, and  $N$  is the number of observations considered to carry out the estimate. Both expressions come from the application of the Maximum Likelihood Estimation to the estimate of the parameters  $(\mu, \sigma)$  of a GBM-type stochastic model.

We can simplify Eqs. (7) and (8) because there is a temporary data series for gas price at a daily frequency, and the time step considered to estimate the parameters  $(\mu, \sigma)$  is 1 day, then  $\Delta t = 1$ . Likewise, we can understand the expression inside the sum of Eq. (7) as the return of the day-to-day gas price normalized to a unit basis. That is, this expression states the gas price's increase or decrease over time expressed on a unit basis. Based on these considerations, we rewrite Eqs. (7) and (8) as follows:

$$R_i = \left( \frac{P_i}{P_{i-1}} - 1 \right), \tag{9}$$

$$\hat{\mu} = \frac{1}{N} \sum_{i=1}^N R_i, \tag{10}$$

$$\hat{\sigma} = \frac{1}{N} \sum_{i=1}^N (R_i - \hat{\mu})^2. \tag{11}$$

From Eqs. (10) and (11), we conclude that the Maximum Likelihood Estimation for drift and volatility can be used to simulate the gas price using GBM in a relatively straight-forward manner. We accomplish this by calculating the arithmetic mean of the unitary returns of the gas price and its variance for a price time series with  $N$  data.

The estimation of these parameters using Eqs. (10) and (11) implies that both drift and volatility are constant over time, which entails the time series of the normalized unitary returns being stationary. A time series becoming mathematically stationary means that the mean and variance are constant over time. We analyze the stationary hypothesis of the historical series of the gas price unitary returns in Fig. 3.

The drift or mean of returns appears to be quite stable and close to zero, without the unit returns showing a trend. However, the volatility or standard deviation of returns is quite variable and depends on the lapse of time considered. The series cannot be considered stationary in the strict sense of the term, as in fact the time series of the returns displays heteroscedasticity or variability in variance, as illustrated in Fig. 3.

Given the characteristics of the structure of the historical data, in order to carry out gas price evolution simulations using GBM, we consider four different scenarios ( $S_i$ ). These include three theoretical scenarios, which consider zero drift, very close to the real average drift, which is found to be in the range of  $10^{-4}$ , and volatilities for 0.5% (on 80.95% of occasions, the gas price returns are greater than or equal to |0.5%|), 1% (on 69.01% of occasions, the gas price returns are greater than or equal to |1%|), and 1.5% (on 57.76% of occasions, the gas price returns are greater than or equal to |1.5%|), respectively; these scenarios are named S1, S2, and S3. Lastly, we include a fourth scenario where we apply the Bootstrapping resampling technique to determine a drift and volatility that are statistically fitted to the historical price series and whose characteristics are covered in further detail in Soage et al. (2024). This scenario is hereinafter referred to as S4 or as the real scenario.

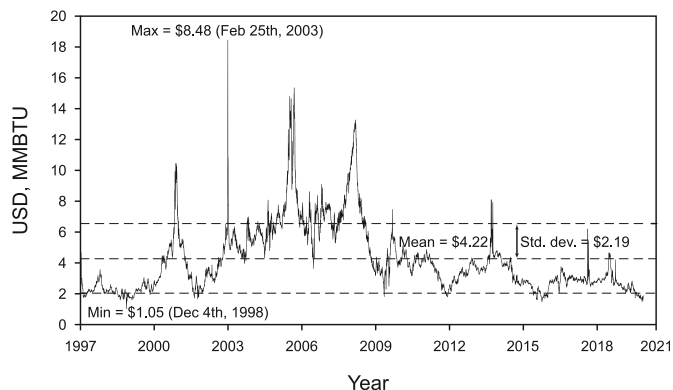


Fig. 2. Gas price listed (HHSP) from the 6th of January 1997 to the 16th of April 2020 (5861 trading days).

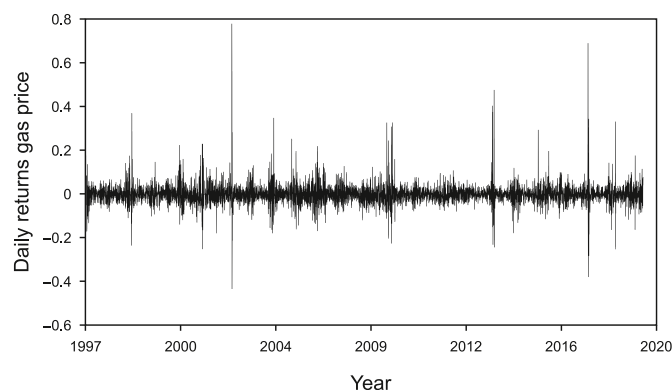


Fig. 3. Gas price daily returns (HHSP) from the 6th of January 1997 to the 16th of April 2020 (5861 trading days).

#### 2.4. Monte carlo simulation combined with GBM to determine numerical gas price distributions

We applied the Monte Carlo simulation combined with the GBM theory to the synthetic generation of gas price trajectories in three scenarios, S1 to S3, in which the drift and volatility remain constant (Hacura et al., 2001; Papadopoulos and Yeung, 2001).

In the historical series, the drift tends to zero and the volatility assumes a low (S1), intermediate (S2) or high (S3) value. The level of the historical appearance of these estimated values is quite high. In other words, scenarios S1 to S3, being theoretical gas price scenarios, are scenarios that are not far from reality. This enabled us to conduct a simpler initial approximation to gas price simulations using GBM.

For each pair of values ( $\mu$ ,  $\sigma$ ), we carried out 1000 price simulations. We used a starting price of  $P_0 = \text{USD } 2.61/\text{MMBTU}$ , corresponding to the closing gas price on the 17th of May 2019 and which corresponds with the price USD 2.71/Mscf. The time step considered is 36.5 days, which involves carrying out 101 calculations (including  $t = 0$  or start price) for each of the simulated trajectories, in order to finish the 10-year period.

We applied Eq. (6) to the indicated gas price and the drift and volatility parameters appearing in Fig. 4, which also shows the outputs obtained for the three proposed scenarios.

We can see in Fig. 4 that if we take an elevated daily volatility, the price values tend to disperse as time evolves. However, for low daily volatilities, the prices tend to concentrate close to the initial value of the simulation when assuming zero drift.

On the other hand, we used the Bootstrapping technique to perform statistical sampling in the HHSP price series and numerically generate a PDF of the  $P_0$ , the drift, and the volatility using Eqs. (7) and (8), or more directly, Eqs. (9)–(11) based on HHSP gas price unit returns. The methodology is described in Soage (2021). With this technique, we created an S4 price scenario in which 1000 price trajectories were generated with a behavior that we consider to be more in line with reality based on historical gas price data (Fig. 5).

We used this set of simulations as a basis for the calculations of the dynamic financial indicators for investment selection that are developed in the following sections of this paper.

#### 2.5. Impact of inflation on dynamic financial indicators for shale gas investments

In economics, inflation is considered as the increase in the price of goods and services over a certain time period. This can be interpreted as a loss in purchasing power of the population in a region caused by a decrease in the value of money (Barro, 1995). It is clear that the value, understood as the purchasing power, of USD 100 in 2022 is very different to the value of the same amount of money in 1980. The difference in the purchasing power to acquire products associated with the same amount of money in the same currency is known as inflation (Sarel, 1996).

There are different interpretations of the effect of inflation on the economy of a country or region. In general, high or very high inflation, known as hyperinflation, generates a loss in purchasing power for the population of the affected region and hence its impoverishment (Hanke and Bushnell, 2017). There are many causes of hyperinflation, such as a political decision to issue large amounts of currency, a market imbalance that results in drastic downward trends in demand, or an increase in the price of goods and services due to a strong increase in production costs. On the other hand, very low or negative inflation, known as deflation, is usually the result of a fall in market demand, i.e., a downward trend in the economy that attempts to compensate for falling market trends by decreasing the prices of goods and services, which, just

like with hyperinflation, leads to the general impoverishment of the population (Mastromatteo and Rossi, 2015).

There is a general consensus among experts on economics and currency theory that the best scenario is growing but contained inflation, which is indicative of both a balanced and constant expansion of both the market and the economy (López-Villavicencio and Mignon, 2011).

Inflation analysis involves different metrics and calculations. The most commonly accepted is the Consumer Price Index (CPI) (Bryan and Cecchetti, 1993). This indicator is calculated by taking a set of frequently consumed goods and services and calculating their value at a given time. At a later time, the value of this set of goods and services is recalculated, and the increase in value is also calculated (positive or negative). This variation is usually expressed as a percentage of annual variation for a given country (Diewert, 1998). The CPI is used as an indicator to estimate inflation, although it is a financial indicator with certain limitations.

For example, it does not consider the variation in the quality of the goods and services, or whether new goods or services should be included, and hence the price comparison loses uniformity. Furthermore, depending on the country, the composition and weighting of sectors from which the goods and services are derived (transport, food, housing, etc.) vary considerably (Lebow and Rudd, 2003). However, despite all of these considerations, it is unanimously adopted as the indicator for measuring a country's inflation (Blinder et al., 1980).

We used inflation data from the USA in this paper for the purpose of analyzing the NPV and IRR (Fama and Gibbons, 1982; Shahsavari et al., 2010). When calculating these two financial indicators (NPV and IRR), inflation is used as a depreciation factor over time for investment cash flow (Goldfajn and Werlang, 2000; Egilsson, 2020).

In Fig. 6, we show the evolution of the annual inflation in the USA from 1914 to 2019 (U.S. Bureau of Labor Statistics, 2022), expressed as a percentage. The annual inflation has remained quite stable since 1990, in the range of 2%–3%, with some downward corrections, like the one in 2009 caused by the financial crisis which resulted in the country entering a period of deflation with a year-on-year inflation value of  $-0.4\%$  (McKibbin and Stoeckel, 2009).

The Bureau of Labor Statistics (BLS) in the USA calculates inflation on a monthly basis, although Fig. 6 shows yearly data. In Fig. 6, we also display the statistical characteristics of this time series. The time period considered is from 1914 to 2019, which involves 106 CPI data (Bryan and Cecchetti, 1993).

We assume that the gas price itself has a certain correlation with inflation, given that this raw material is a listed asset of growing importance within the USA consumables market, especially because of its use in generating electricity (Energy Information Administration (EIA), 2016). In line with this idea, we correlated gas price variations (gas inflation) between 1997 and 2019 with the inflation data from the USA for the same time period. To carry out this correlation analysis, we took HHSP quote data on a yearly basis, and the year-to-year gas price inflation was calculated.

The best polynomial fit that we obtained correlates global inflation and gas inflation with a Pearson coefficient of  $R^2 = 0.5012$  (Fig. 7(a)). Although this correlation is weak, it is not negligible. This correlation is stronger for larger or smaller rates of gas price inflation. It makes sense that periods of extreme gas prices coincide with extremes of overall inflation, as gas prices can be used as a proxy for energy consumption and economic output (Fig. 7(a)).

According to the U.S. Energy Information Administration (EIA), in 2021, gas became the main source of electricity production in the USA, reaching 38.3% of total production, followed by coal at 21.8% and nuclear power at 18.9% (Energy Information Administration

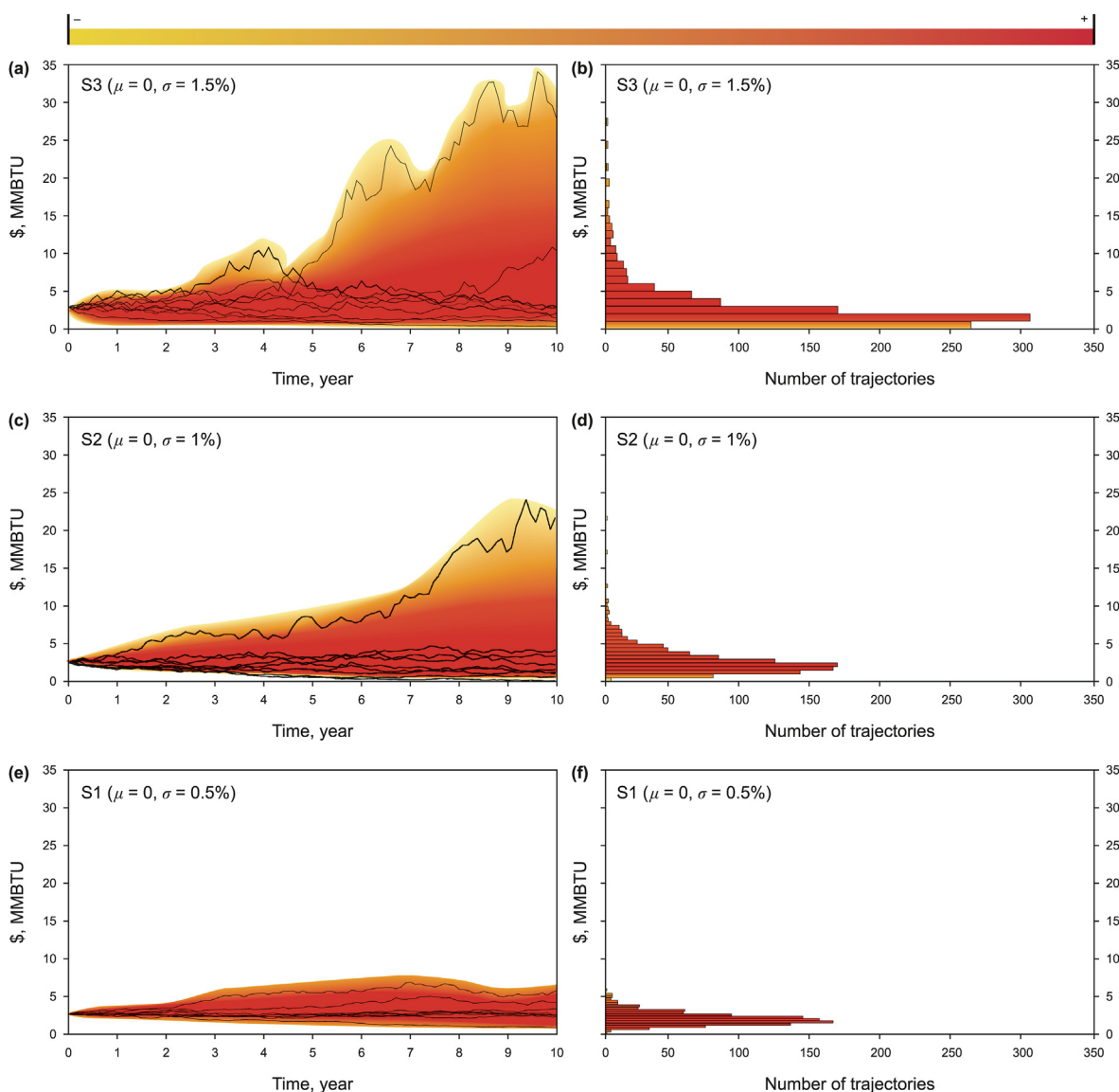


**Fig. 4.** (a) 10 of the 1000 price evolution simulations for scenario S3 are shown: maximum value, minimum value, and 8 random intermediate trajectories. A price density map is also presented, with trajectory concentrations indicated by warm colors; dark red indicates high concentration and bright yellow indicates low concentration. (b) Histogram of price frequencies for scenario S3 at the end of the 10-year period. (c) Price density map for 1000 realizations of price evolution in scenario S2. (d) Histogram of price frequencies for scenario S2 at the end of the 10-year period. (e) Price density maps for 1000 realizations of price evolution in scenario S1. (f) Histogram of price frequencies for scenario S1 at the end of the 10-year period.

(EIA, 2022a, 2022b). This trend indicates that the importance of gas tends to increase over time, given that in 2001 gas consumption for electricity generation was up 17.11% (Energy Information Administration, 2022a). These data suggest that this general inflation vs. gas inflation correlation will be increasingly strong (Energy Information Administration, 2016).

Based on the price series we generated for scenarios S1 to S4, the annual gas inflation can be calculated using Eq. (12), expressed as a percentage. The calculation is carried out on an annual basis, as the time step of the generated series or  $\Delta t$  is 1.2 months or 36.5 days, so in order to annualize the calculation, the gas returns must be raised to the power of 10 ( $10 \times 1.2$  months = 12 months or 1 year;  $10 \times 36.5$  days = 365 days or 1 year).

Using Eqs. (13) and (14), as well as values of the stochastic gas price trajectories, we can obtain the daily inflation. This derivation process combines concepts of compound interest with empirical data obtained from the corresponding regression.

In Eqs. (12)–(14), the term  $CPI_{gas\ y}$  refers to yearly gas inflation,  $CPI_d$  refers to daily US global inflation, and  $CPI_y$  to yearly US global inflation. This mathematical approach for each time interval of the different price simulations carried out in scenarios S1 to S4 provides a daily inflation that correlates with the gas price data. This enables dynamic financial estimators to be calculated for shale gas wells, thereby providing a realistic approximation for the natural gas market.

$$CPI_{gas\ y}(t) = \left( \left( \frac{P_{gas}(t + \Delta t)}{P_{gas}(t)} \right)^{100} - 1 \right) \times 100 \tag{12}$$

$$CPI_y = 2.374 + 0.009475 \times CPI_{gas\ y} - 0.000424 \times CPI_{gas\ y}^2 + 5.27 \times 10^{-6} \cdot CPI_{gas\ y}^3$$

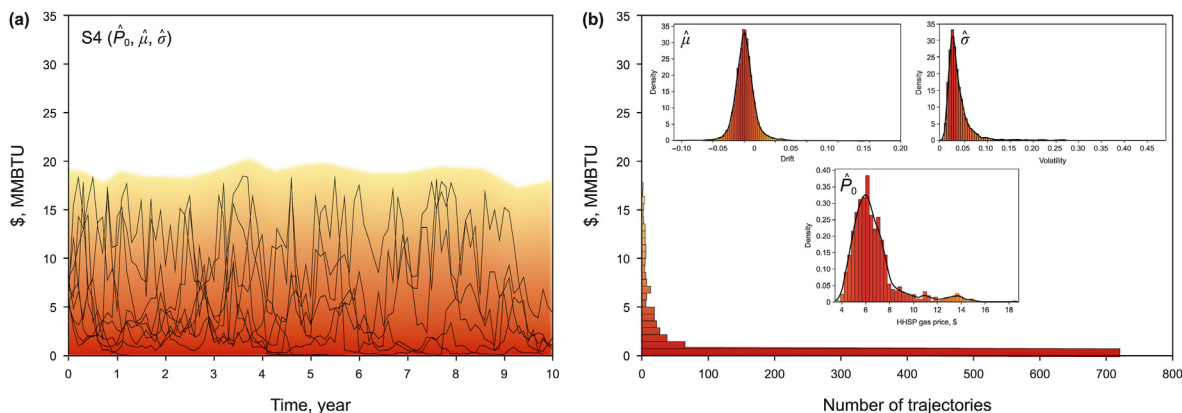


**Fig. 5.** (a) Examples of realizations and price density maps for 1000 realizations of price evolution in scenario S4. 10 of the 1000 simulations are shown: maximum value, minimum value, and 8 random intermediate values. Concentration of trajectories is indicated using warm colors; dark red for high concentration and bright yellow for low concentration. (b) Histogram of price frequencies for scenario S4 at the end of the 10-year period.

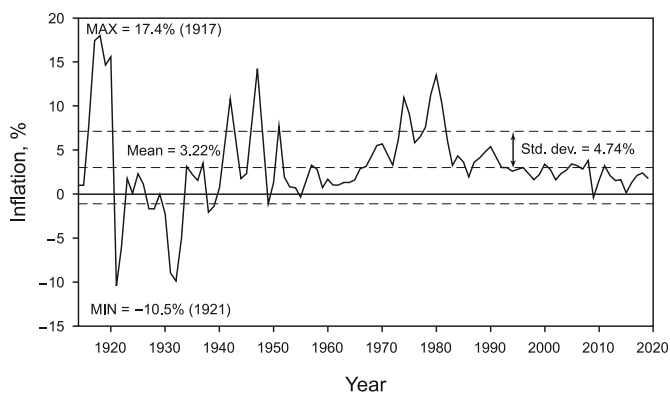


**Fig. 6.** USA year-on-year inflation (1994–2019); 106 CPI values, data expressed as percentages. Source: Bureau of Labor Statistics (BLS), USA.

$$CPI_d = \sqrt[365]{1 + CPI_y - 1} \tag{13}$$

In Fig. 7(b), we show the history of 10 inflation trajectories taken randomly from the 1000 realizations for scenario S3. We also draw the frequency distribution for the 1000 realizations on a warm color scale.

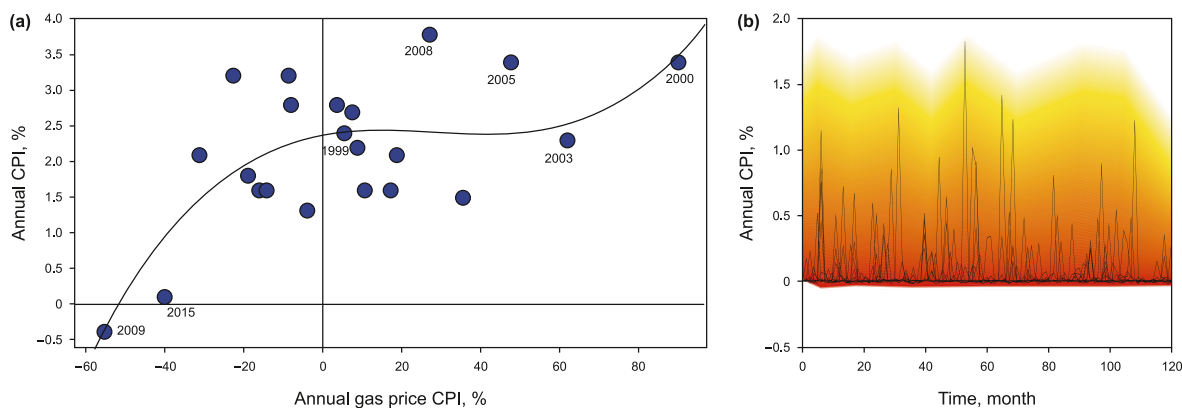


**Fig. 7.** (a) Polynomial correlation between gas price inflation and global inflation in the USA (22 years of data, from 1998 to 2019). The year is indicated for some data. (b) Annualized global inflation expressed as % for 10 outputs of 1000 totals simulated in scenario S3. Black lines represent 10 of the 1000 generated Annual CPI trajectories. The warm color scale indicates where the higher concentration of inflation trajectories is located.

## 2.6. NPV and IRR as statistical financial estimators applied to shale gas

### 2.6.1. Introduction

We used two financial indicators in this study, each one having its advantages and disadvantages when it comes to making financial decisions (Ranasinghe and Russell, 2006; Weijermars, 2013). The net present value (NPV) is one of the most commonly used financial indicators in the world of energy, O&G, and, in particular, shale gas (Bas, 2013). This indicator calculates the final value of an investment after a defined period of time, considering the cash flows produced by the investment, the depreciation in the value of money, the operational expenditures (OPEX), royalties and taxes, and the initial investment or CAPEX. It is a financial indicator that is very commonly used to evaluate investments involving fixed assets, large sums of money, and long useful lifespans.

The NPV can have the following values:

- NPV > 0 indicates a feasible investment, meaning that its value at the end of the operating lifespan will be positive. In general, the higher the NPV, the more attractive the investment.
- NPV = 0 indicates a financially neutral investment.
- NPV < 0 indicates an unprofitable investment that should not be undertaken.

The internal rate return or IRR is the discount rate value that yields an NPV of zero. Another way to define it is to consider it as

the interest rate at which the cash flows equal the value of the investment made. It is possibly the closest financial indicator to the commonly used concept of the profitability of a financial product like an investment fund or government bond. Any IRR of an investment that exceeds that expected for a financial product considered safe makes the investment appear attractive. Another way to analyze this indicator is to check if the IRR obtained in the investment analysis is greater than the expected depreciation. If this is the case, it can also be considered a viable investment.

Both the NPV and IRR have been used in the study of shale gas investments (Lake et al., 2013; Yu and Sepehrnoori, 2013).

### 2.6.2. Methodology to obtain statistical net present value (NPV)

The NPV is a dynamic financial indicator defined by studies as the cash flow value for a determined investment, updated to the present moment in time (Soage et al., 2021).

We may express the NPV mathematically as shown in Eq. (14). This formula uses classical terminology in the O&G industry regarding asset evaluation:

$$NPV = \sum_{i=1}^N \frac{(1 - \text{RateT}) \cdot (P_{\text{gas}}(i) \cdot \text{Mscf}(i) \cdot (1 - \text{Roy}) - \text{OPEX})}{(1 + \text{CPI}_{\text{d}}(\text{CPI}_{\text{gas y}}(i)))^i} - \text{CAPEX}. \quad (14)$$

The terms appearing in Eq. (14) are defined as follows:

- CAPEX, or “capital expenditure”, is the financial value of the investment in the shale gas well expressed in US dollars. In this model, we consider a shale gas well with a CAPEX of USD 4.8 MM.
- $i$  is the time step.
- $N$  is the total number of time steps.
- $P_{\text{gas}}(i)$  is the gas price in the time step  $i$ ; value is expressed in USD/Mscf.
- $\text{Mscf}(i)$  is the flow rate at time step  $i$ ; value is expressed in Mscf/d. When this value is multiplied by  $P_{\text{gas}}(i)$ , the gross cash flows for time step  $i$  are obtained.
- Roy refers to royalties, expressed on a unit basis, paid to the owner of the land and other agents such as county administrations in some cases. We assume a flat rate of 15% of the gross economic flow.
- OPEX, or “operational expenditures”, are the well’s operating costs. We consider a constant day-to-day cost value of USD 150/day. It is sometimes expressed in units of USD/Mscf, showing that its importance decreases as gas production drops.
- $\text{CPI}_{\text{gas y}}(i)$  is the annualized gas price inflation expressed on a unit basis and varies with each time step.
- $\text{CPI}_{\text{d}}$  reflects daily inflation and depends on the annualized gas price inflation.
- RateT represents the profit taxes expressed on a unit basis. We apply a 21% tax rate, which is the current gross rate for corporate tax in the USA.
- We assume that all costs are included in the mathematical formulation reflected in Eq. (14).

We used Monte Carlo simulation to estimate the PDF of the NPV. We applied Eq. (14) by combining the price trajectories of each scenario (S1–S4) with the gas production curves of the parametric sweep performed in (Soage, 2021) and (Soage et al., 2021). This generated, for each value of the parameter studied (e.g., porosity = 2.5%) and for a specific scenario (e.g., S2), 1000 different

NPVs. This means that the gas price data series obtained were paired with consecutive production data. It is not possible to match price data with production data in a random manner since the gas price series has a certain internal structure that must be preserved. Finally, we fitted a non-parametric PDF to each set of NPVs using the kernel density estimation (KDE) method.

To be precise, the methodology used is as follows:

- We take the base case of a shale gas well (Soage, 2021; Soage et al., 2021), along with the production curves calculated deterministically via numerical modeling, based on the mathematical model that describes the phenomenon of shale gas production.
- We select one of the parameters that was subject to analysis, e.g., porosity, and we take production curves for each value of this studied parameter.
- We combine price scenarios S1 to S4 with each production curve obtained for each parameter value.
- For each parameter value and each price scenario, we use 1000 price realizations to calculate 1000 NPVs.
- With the distribution of NPVs for a specific value of a parameter and a specific scenario, we adjust a non-parametric PDF of Gaussian kernels using the KDE method. We perform a K-S test to check for an acceptable significance level (in general above 5%) and enable probabilistic NPVs to be calculated.
- We calculate the 10%, 50%, and 90% percentiles of the NPV (P10, P50, and P90) for every density function.
- We show the percentages indicated on a graph according to the studied parameter as its value changes.

We illustrate this methodology in Fig. 8. In Fig. 8(a), we show 10 sample realizations (of the 1000 carried out) for the cash flow of a well with 3% porosity considering scenario S3. We also include the time evolution of the NPV for 10 sample realizations of 1000 calculated based on the previous cash flows (Fig. 8(b)). Furthermore, we present the probability distribution to NPV for each porosity value studied within scenario S3 and with their corresponding P10, P50, and P90 (Fig. 8(c)). The NPV frequency distributions overlap for porosities of 1% and 3% (insets in Fig. 8(c)).

Fig. 9 summarizes the results obtained by combining the parametric variations in porosity, induced permeability, kerogen content, and ellipsoidal fracture volume or effective propped volume (EPV) geometry with each of the analyzed scenarios, S1 to S4. The insets in the figure indicate the statistical significance levels obtained for each non-parametric function adjusted using the KDE method and the corresponding bandwidth of each Gaussian kernel. The bandwidth is normalized by dividing its value by the investment CAPEX, resulting in a bandwidth normalized to a scale of 0–1. The aspect ratio (AR) is a dimensionless value that relates the two horizontal axes of the hydrofractured ellipsoid. AR values range from 0.05 to 7.50. In this figure, in order to improve the understanding of the graphics, we represent AR according to the value of the semi-axis  $a$ . The calculation of the semi-axis  $a$  with the value of the AR is explained in (Soage et al., 2021).

### 2.6.3. Methodology to obtain statistical internal rate return (IRR)

The mathematical formula to calculate the IRR applied in the analysis carried out in this paper is presented in Eq. (15). The formulation of this equation aligns conceptually with the idea that the IRR is the maximum discount rate, after which an investment is no longer profitable. Hereinafter, we consider the IRR the value of profitability in its most commonly used sense.

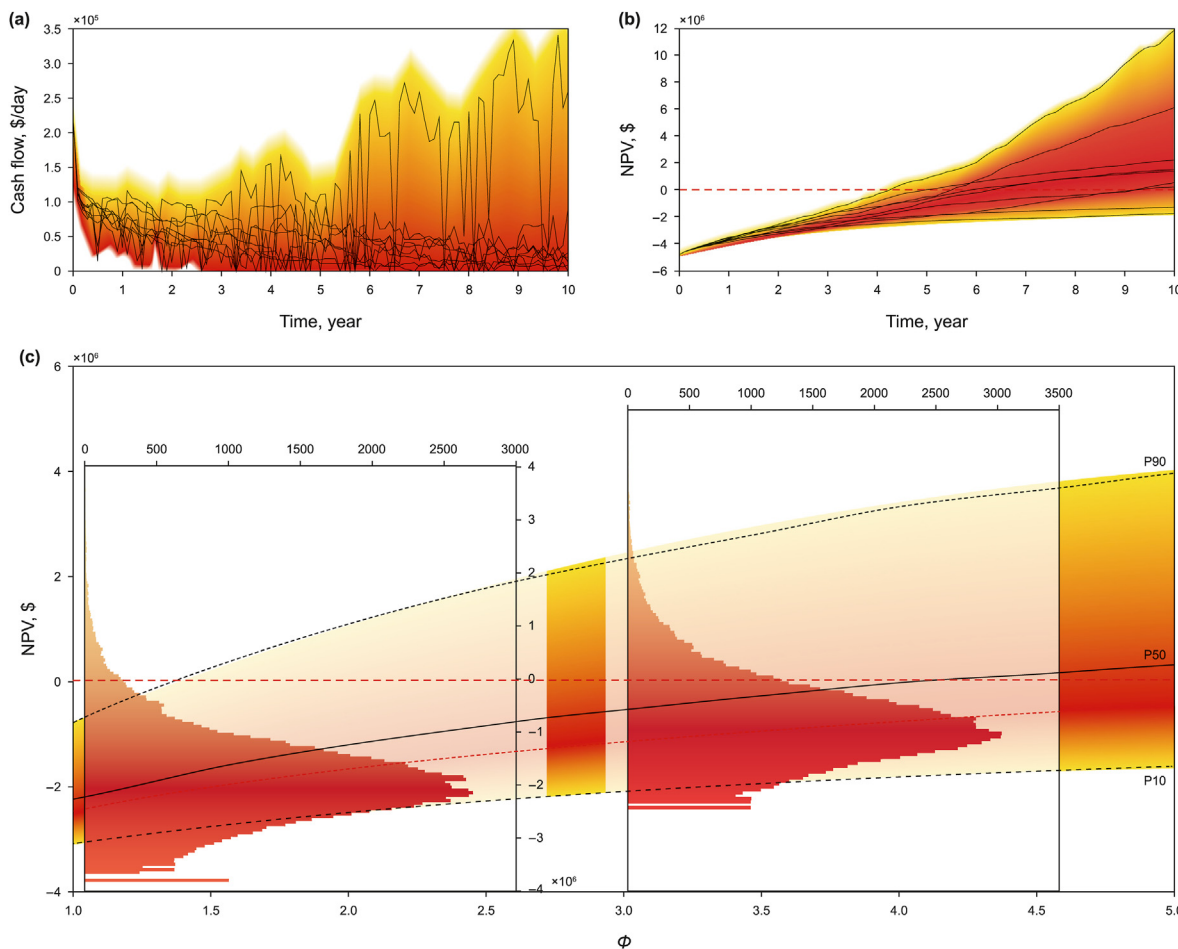


**Fig. 8.** (a) Cash flow evolution over time for 10 price trajectories. Warm colors represent areas with the greatest accumulation of cash flow trajectories. This calculation is for the gas production curve with 3% porosity and price scenario S3. (b) Time evolution of NPVs corresponding to the cash flows in (a). The relevant NPV is at the end of the 10-year operating period of the shale gas well. (c) Results of P10, P50, and P90 NPV percentiles at 10 years for the base case in scenario S3. Areas with the greatest accumulation of realizations are shown using warm colors. NPV histograms for porosities of 1% and 3% are inset to illustrate graph design.

$$0 = \sum_{i=1}^N \frac{(1 - \text{RateT}) \cdot (P_{\text{gas}}(i) \cdot \text{Mscf}(i) \cdot (1 - \text{Roy}) - \text{OPEX})}{(1 + \text{IRR})^i} - \text{CAPEX}. \tag{15}$$

An important mathematical aspect of the IRR's calculation is that it can take multiple values depending on the cash flow's evolution. The origin of this mathematical phenomenon is that the IRR is a polynomial expression with multiple roots (as many as the degree of the polynomial). These roots can be real or complex. The most common and desirable situation is that there is only one real root, and the remaining roots are complex. However, the polynomial coefficient structure does not always provide this result. In the event of multiple roots, we take the lowest positive real root as the IRR. If there are no positive roots, we take the greatest negative value. In the case where there are no real roots, it is considered that the IRR does not exist for the mathematical structure that defines the investment.

For the statistical calculation of the IRR, we used the same methodology described in Section 2.6.2 of this article. Fig. 10 shows a summary of the results for different simulations where the production curves of the parametric sweeps cross with the gas price data considered for the different theoretical price scenarios S1–S4.

### 3. Results and discussion

In this study, we generally consider the value of the financial indicator for the P90 percentile as a measure of success. Likewise, we consider as a risk measure the value of the financial indicator for the P10 percentile.

#### 3.1. Statistical net present value results

In Fig. 9, we show the results obtained for the calculation of the NPV in shale gas investments. We point out our key findings below.

As the volatility increases going from scenario S1 to S4, the dispersion of the NPVs increases considerably with the increase in the parameter values. In the shale gas extraction sector, success during periods of high volatility is strongly dependent on having suitable petrological and design parameters. As an example, for a permeability of 10  $\mu\text{d}$ , we obtain an NPV of USD 2.7 MM (Fig. 9 permeability vs. S4). As the volatility increases, so does the financial risk, so for the previous example, the P10 falls to a negative NPV of nearly USD –4 MM. The most relevant parameters for the financial viability of a shale gas well as defined in the base case of (Soage et al., 2021) are in the following order: porosity, induced permeability, ellipsoidal fracture geometry (EPV shape), and kerogen content. We establish relevance based on the sensitivity of the NPV percentiles to the variation in the parameters.

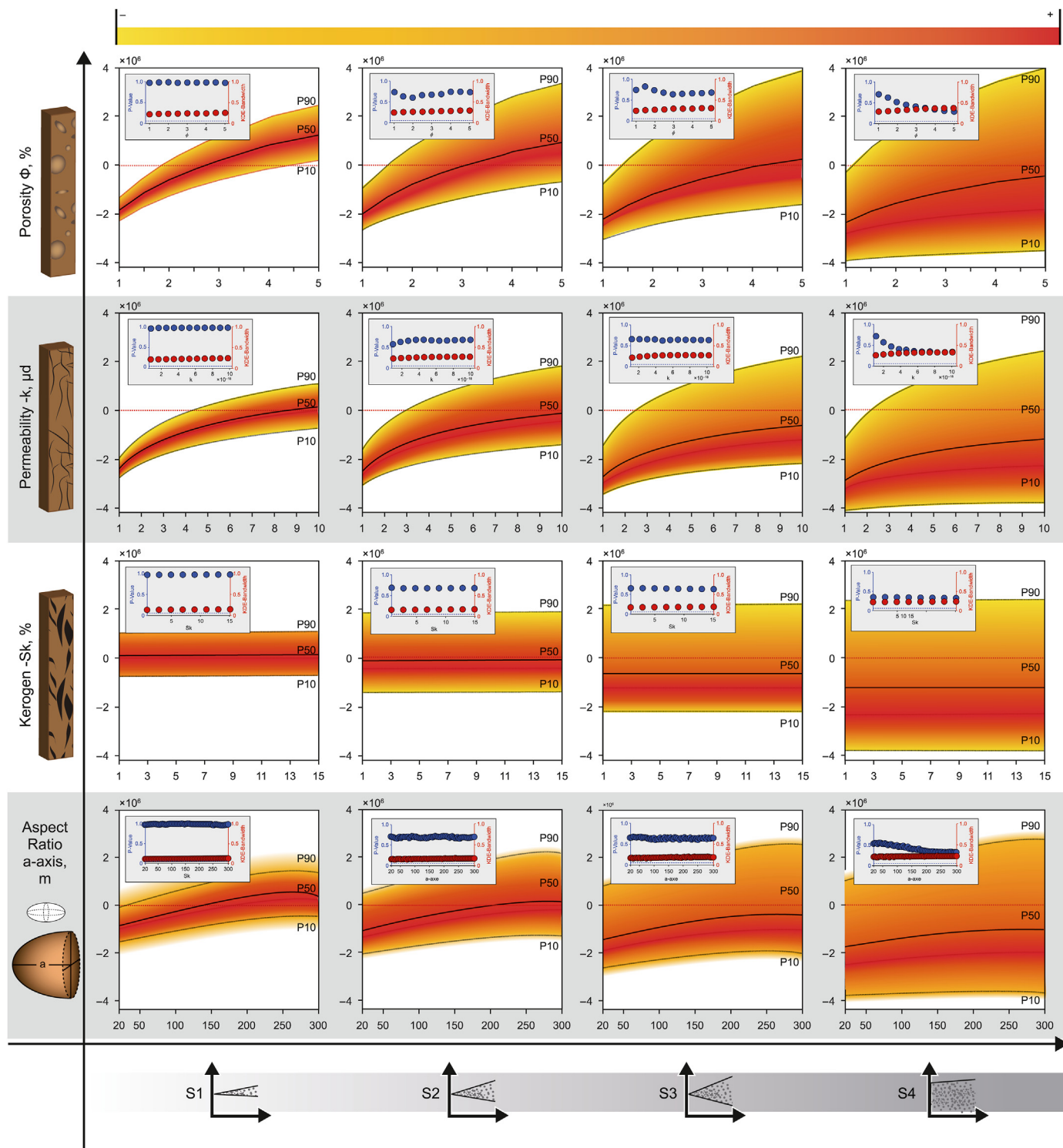
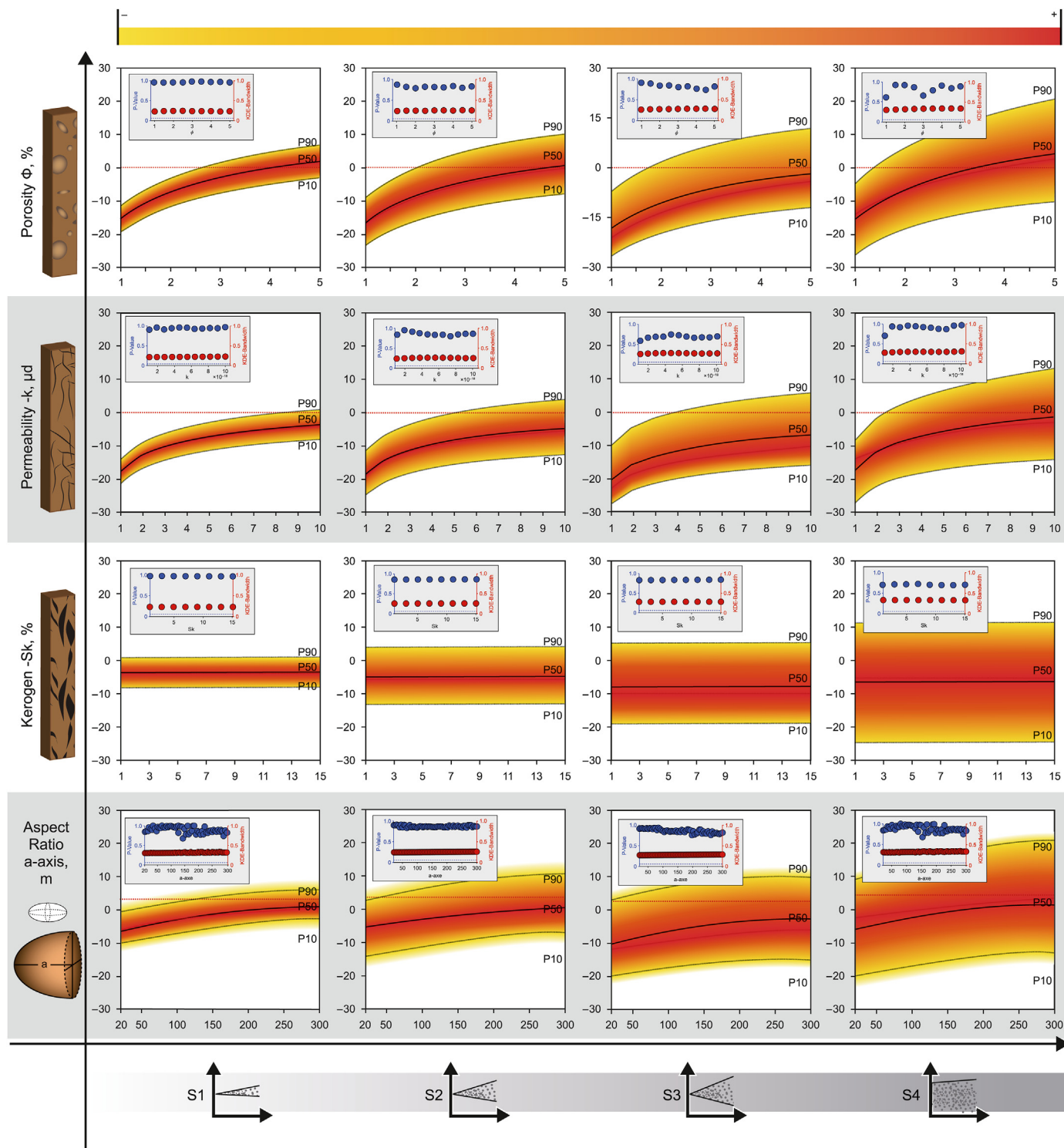


Fig. 9. NPV (USD) results are presented in matrix form. The vertical axis shows variations in gas production parameters, and the horizontal axis shows different price scenarios (S1 to S4). The P10, P50, and P90 percentiles are shown for each result, with higher concentration areas in red and lower concentration areas in yellow using a warm color scale. Each result includes a graph with the statistical significance of the nonparametric PDF adjustment (blue dots) on a 0 to 1 scale and the bandwidth normalized by the CAPEX of the Gaussian kernels used to adjust the PDF (red dots).

### 3.2. Statistical internal rate return value results

We observe similar results to those of the NPV case study. Increasing dispersion was observed in the IRR values with an increase in volatility and/or in the production parameters, a growth

in the risk of investment failure (i.e., a fall in the IRR P10 value), and an increase in the probability of success (increase in IRR P90 value). The most relevant parameters for the financial viability of a shale gas well, as defined in the base case (Soage et al., 2021), are in the same order as in the NPV study: porosity, induced permeability,



**Fig. 10.** IRR (%) results. Analysis presented in matrix form. The vertical axis represents the variations in the gas production parameters. The horizontal axis represents the different price scenarios, S1 to S4. The P10, P50, and P90 percentiles are represented for each result, and the areas with a higher concentration (red) and lower concentration (yellow) of realizations are shown using a warm color scale. Each result includes a graph with the statistical significance of the nonparametric PDF adjustment (blue dots) on a 0 to 1 scale and the bandwidth normalized by the CAPEX of the Gaussian kernels used to adjust the PDF (red dots).

EPV geometry, and kerogen content. We compared the results of the percentiles of the NPVs with those of the percentiles of the IRRs, and we observed that the behavior of both indicators is slightly different. The IRR is a financial indicator that is more sensitive to parametric variation, but less sensitive to price volatility.

### 3.3. General discussion

We studied different price scenarios. Scenarios S1 to S3 were generated considering a constant drift and an increasing volatility of 0.5% for S1, 1% for S2, and 1.5% for S3. On the other hand, S4 is a

scenario based on statistical estimators whose PDF has been calculated using the Bootstrapping statistical resampling method applied to the historical gas price series. We observed that for a greater price volatility, the P90 and P10 percentiles of the NPV and IRR financial estimators tend to diverge. The greater the volatility, the greater the dispersion between percentiles. This indicates a greater success value (P90). However, there is also an increase in risk as the P10 falls, entering into negative NPV or IRR values.

We also observed that the greater the expectation of a positive result, statistically, the greater the risk. In this regard, shale gas well investments respond to a risk–profit balance that is characteristic of classical financial products.

The comparison between the results obtained for S1–S3, in which the constant gas price is considered throughout the life of the investment, and for S4, in which the gas price varies during the gas extraction, allow us to show that both the success and the risk assumed in shale gas investments are underestimated.

The financial estimators' (NPV or IRR) percentile values increase monotonically as the petrophysical and design parameters increase in their values. The maximum P90, P50, or P10 are reached for the maximum value of those parameters.

We used the final results of the financial estimators to analyze shale gas investments. We could thus rank the economic importance of the parameters in shale gas economic performance. In order of importance, the first factor is the gas price, which plays a key role in the financial performance of a shale gas investment. The price at the start of the investment, the volatility, and the drift price are determining factors in the final result of the investment. In second place are production parameters such as induced permeability or EPV geometry. The least dominant parameters are the petrological factors like porosity or kerogen content. We will discuss the kerogen content parameter in more detail. The amount of methane adsorbed in the kerogen is described by the Langmuir isotherm model (Yu et al., 2016). This model consists of a rational function that has two parameters that are determined experimentally, i.e., Langmuir pressure and Langmuir volume. The value of the parameters is intrinsically determined by the origin of the organic matter from which the kerogen comes. We adopted parameters such that its contribution of methane is low in relation to the methane contributed by the pore methane (Zhao et al., 2018). The Langmuir pressure marks the pressure at which half of the adsorbed gas has been released into the pore space of the rock matrix. In this case, this pressure is 3 MPa, while the minimum pressure reached by the SRV in the simulations does not go below 5 MPa. This indicates that most of the methane has not been released. Although the amount of kerogen increases considerably, the net contribution of gas is low, and for this reason, this petrological parameter has little importance in financial performance.

We show some quantitatively noteworthy results. We focus this analysis on NPV results of the scenario S4 and maximum parameter values. The P90 NPV oscillates between approximately USD 2.3 MM and USD 4 MM. The CAPEX of the base case shale gas well is USD 4.8 MM. This explains the great expansion of this gas production method. Likewise, the financial risk quantified for the P10 NPV oscillates between approximately USD –3.8 MM and USD –4 MM. Although this is a high-risk scenario, when compared with the success value (P90), it is very acceptable for the indicated CAPEX investment.

We studied the IRR from a quantitative perspective, as in the previous analysis of the NPV. The IRR P90 values fall between 12% and 21%. This is a profitable investment and high above the value that any common financial product can offer. On the other hand, the IRR P10 oscillates between –25% and –10%. This is a considerable risk, albeit in agreement with the statistically expected success.

These results may be extended to more complex studies like

optimizing shale gas well portfolios or purchasing shale gas wells according to their statistical value.

Summarizing this discussion, it can be stated that a stochastic approximation of the financial parameters of shale gas wells enables a more complete analysis of these types of investments, allowing a rigorous understanding of the economic values that can be obtained with shale gas investments and the risks that these investments entail. The trajectories of the companies that have been dedicated to this business show a trend of behavior that reflects the results exposed in this discussion: great business successes combined with tragic bankruptcies. In addition, as a result of the study, it can be verified that the good petrophysical values (e.g., high porosity value) and a good well design (e.g., hydrofracturing geometry) are essential, but not easy to achieve. This leads us to intuit a scientific explanation for the so-called “sweet spot” theory, according to which shale gas wells with good economic performance tend to accumulate in certain areas of a play. This study shows that this must be the case since the requirements to achieve a good investment require a multiparametric combination (porosity, induced permeability, kerogen content, and fracture geometry) that may be scarce in the reality of the geological plays and requires numerical or data-analytics-based optimization techniques for its determination in the field (Cristancho-Albarracin et al., 2017; Psarras et al., 2017).

#### 4. Conclusions

The most important conclusions for our study are as follows:

- We proposed a methodology that, using Monte Carlo simulation, combines numerical modeling and stochastic process modeling to obtain statistical financial estimators in PDF form. This allows us to calculate the values of the estimators with a probability of occurrence.
- The application of this methodology to shale gas investments allows for determining the most relevant investment parameters.
- The incorporation of the gas price variability during the life of a shale gas well provides a better understanding of the high profits and risks of this activity.
- Considering gas price variability as another key variable is essential for industrial operators. In particular, price volatility is the key factor that determines the profit/risk level of an investment.
- At very high price volatilities, the profit percentiles rise, but so do the loss percentiles. This result shows that investments in shale gas behave like a classic investment: high risk–high profit. This conclusion is not intuitive since shale gas production is governed by natural physical processes.
- We observe that for any of the financial parameters studied, the loss percentile (P10) remains increasingly insensitive as the petrological and design parameters improve. This result is not evident and has its origin in the restriction that the prices of commodities cannot take negative values.
- The NPV and IRR were calculated with a probability of occurrence. This is a new approach in shale gas investments, where static price values are usually considered which do not allow the quantification of investment risk.

#### Declaration of competing interest

The authors declare that they have no known competing financial interests or personal relationships that could have appeared to influence the work reported in this paper.

## CRedit authorship contribution statement

**Andres Soage:** Writing – original draft, Visualization, Methodology, Investigation, Data curation, Conceptualization. **Luis Ramirez:** Writing – review & editing, Funding acquisition. **Ruben Juanes:** Writing – review & editing, Validation. **Luis Cueto-Felgueroso:** Writing – review & editing, Validation, Project administration, Formal analysis, Conceptualization. **Ignasi Colominas:** Writing – review & editing, Validation, Supervision, Funding acquisition.

## Acknowledgement and funding

This research was partially funded by Government of Spain, Ministry of Science, Innovation and Universities (grant: RTI2018-093366-B-I00), by Government of Spain, Ministry of Universities (grant: Subsidies to Public Universities for the Requalification of the Spanish University System, “Margarita Salas” Grants Modality for the Training of Young Doctors, RD 289/2021 of April 20), by the Xunta de Galicia, Consellería de Educación e Ordenación Universitaria (grant:#ED431C 2018/41), and by the Group of Numerical Methods in Engineering of the Universidade de A Coruña.

## References

Armeanu, D., Lache, L., 2009. The NPV Criterion for valuing investments under uncertainty. *Econ. Comput. Econ. Cybern. Stud. Res.* 4 (4). URL: [https://www.researchgate.net/publication/288787598\\_The\\_NPV\\_Criterion\\_for\\_valuing\\_investments\\_under\\_uncertainty](https://www.researchgate.net/publication/288787598_The_NPV_Criterion_for_valuing_investments_under_uncertainty).

Bai, Y., Meng, J., Meng, F., Fang, G., 2013. Stochastic analysis of a shale gas investment strategy for coping with production uncertainties. *Energy Pol.* 144, 111639. <https://doi.org/10.1016/j.enpol.2020.111639>.

Barro, R.J., 1995. Inflation and Economic Growth. National Bureau of Economic Research, pp. 1–36. <https://doi.org/10.3386/w5326>, 5326.

Barro, R.J., 2015. The stock market and investment. *Rev. Financ. Stud.* 3 (1), 115–131. <https://www.jstor.org/stable/2961961>.

Bas, E., 2013. A robust approach to the decision rules of NPV and IRR for simple projects. *Appl. Math. Comput.* 219, 5901–5908. <https://doi.org/10.1016/j.amc.2012.12.031>.

Bhandari, S.B., 1985. Discounted payback period. *Journal of Financial Education* 14, 1–16. <https://www.jstor.org/stable/41948078>.

Blinder, A.S., Triplett, J.E., Denison, E., Pechman, J., 1980. The Consumer price index and the measurement of recent Inflation. *Brookings Pap. Econ. Activ.* (2), 539–573. <https://doi.org/10.2307/2534330>.

Bryan, M.F., Cecchetti, S.G., 1993. The Consumer Price Index as a Measure of Inflation. National Bureau of Economic Research, pp. 1–23. <https://doi.org/10.3386/w4505>. Working Paper Series 4505.

Cano, A.F., Andrés, F., 2010. Continuous Time Models in Corporate Finance. Master SC Finance, EAFIT-School of Administration, Finance and Technological Institute. URL: <http://hdl.handle.net/10784/11993>.

Chebeir, J., Geraili, A., Romagnoli, J., 2017. Development of shale gas supply chain network under market uncertainties. *Energies* 10 (2), 246. <https://doi.org/10.3390/en10020246>.

Chen, Z., Osadetz, K.G., Chen, X., 2015. Economic appraisal of shale gas resources, an example from the Horn River shale gas play, Canada. *Petrol. Sci.* 12, 712–725. <https://doi.org/10.1007/s12182-015-0050-9>.

COMSOL Multiphysics, 2018. Introduction to COMSOL Multiphysics. COMSOL Multiphysics, Burlington, MA, USA.

Cooper, J., Stamford, L., Azapagic, A., 2018. Economic viability of UK shale gas and potential impacts on the energy market up to 2030. *Appl. Energy* 215, 577–590. <https://doi.org/10.1016/j.apenergy.2018.01.058>.

Cristancho-Albarracín, D., Akkutlu, I.Y., Criscenti, L.J., Wang, Y., 2017. Shale gas storage in kerogen nanopores with surface heterogeneities. *Appl. Geochem.* 84, 1–10. <https://doi.org/10.1016/j.apgeochem.2017.04.012>.

Curtis, J.B., 2002. Fractured shale-gas systems. *AAPG (Am. Assoc. Pet. Geol.) Bull.* 86 (11), 1921–1938. <https://doi.org/10.1306/61EEDDBE-173E-11D7-8645000102C1865D>.

Damodaran, A., 2008. Return on capital (ROC), return on invested capital (ROIC) and return on equity (ROE): measurement and implications. *Social Science Research Network (SSRN)*. <https://doi.org/10.2139/ssrn.1105499>.

Diewert, W.E., 1998. Index number issues in the consumer price index. *J. Econ. Perspect.* 12 (1), 47–58. <https://doi.org/10.1257/jep.12.1.47>.

Dittmar, R.F., Yuan, K., 2008. Do sovereign bonds benefit corporate bonds in emerging markets? *Rev. Financ. Stud.* 21 (5), 1983–2014. <https://doi.org/10.1093/rfs/hhn015>.

Dorfman, R., 1981. The meaning of internal rates of return. *J. Finance* 36 (5), 1011–1021. <https://doi.org/10.1111/j.1540-6261.1981.tb01072.x>.

Drouven, M.G., Grossmann, I.E., Cafaro, D.C., 2017. Stochastic programming models for optimal shale well development and refracturing planning under uncertainty. *AIChE J.* 63 (11), 4799–4813. <https://doi.org/10.1002/aic.15804>.

Egilsson, J.H., 2020. How raising interest rates can cause inflation and currency depreciation. *J. Appl. Econ.* 23 (1), 450–468. <https://doi.org/10.1080/15140326.2020.1795526>.

Energy Information Administration (EIA), 2022a. Electricity explained. Electricity in United States. URL: <https://www.eia.gov/energyexplained/electricity/electricity-in-the-us.php>.

Eshkalak, M.O., Aybar, U., Sepehromori, K., 2014. An economic evaluation on the refracturing treatment of US Shale Gas Resources. In: *SPE Easter Regional Meeting*, Charleston, WV, USA. SPE 171009-MS. <https://doi.org/10.2118/171009-MS>.

Energy Information Administration (EIA), 2022b. Frequently asked questions (FAQS). URL: <https://www.eia.gov/tools/faqs/>.

Energy Information Administration (EIA), 2016. Trends in U.S. Oil and natural gas upstream Costs. URL: <https://www.eia.gov/analysis/studies/drilling/>.

Fama, E.F., Gibbons, M.R., 1982. Inflation, real returns and capital investment. *J. Monetary Econ.* 9 (3), 297–323. [https://doi.org/10.1016/0304-3932\(82\)90021-6](https://doi.org/10.1016/0304-3932(82)90021-6).

Fama, E.G., 1970. Efficient capital markets: a review of theory and empirical work. *J. Finance* 25 (2), 383–417. <https://doi.org/10.2307/2325486>.

Gallo, A., 2014. A refresher on net present value. *Harv. Bus. Rev.* URL: <https://hbr.org/2014/11/a-refresher-on-net-present-value>.

Gimeno, I., 2018. Stochastic modeling to make predictions of the underlying BANKIA (BKIA.MC) of the IBEX-35. Degree Project, Administration and Management - Polytechnic University of Valencia (in Spanish). <https://riunet.upv.es/handle/10251/71966>.

Goldfajn, I., Werlang, S.R.C., 2000. The pass-through from depreciation to inflation: a panel study. In: *Social Science Research Network, Banco Central Do Brasil Working Paper (SSRN)*. <https://doi.org/10.2139/ssrn.224277>.

Hacura, A., Jadamus-Hacura, M., Kocot, A., 2001. Risk analysis in investment appraisal based on the Monte Carlo simulation technique. *Eur. Phys. J. B* 20, 551–553. <https://doi.org/10.1007/PL00011147>.

Haley, C.W., Schall, L.D., 1973. Theory of financial decisions. *J. Finance*. <https://doi.org/10.2307/2978620>.

Hanke, S.H., Bushnell, C., 2017. On measuring hyperinflation. *Venezuela's episode*. *World Economic Journal* 18 (3), 1–18. URL: <https://sites.krieger.jhu.edu/iae/files/2018/02/Hanke-Bushnell-Venezuela.pdf>.

Hong, B., Li, X., Song, S., Chen, S., Zhao, C., Gong, J., 2020. Optimal planning and modular infrastructure dynamic allocation for shale gas production. *Appl. Energy* 261, 114439. <https://doi.org/10.1016/j.apenergy.2019.114439>.

Johar, K., Carmichael, D.G., Balatbat, M.C.A., 2010. A study of correlation aspects in probabilistic NPV analysis. *Eng. Econ.* 55 (2), 181–199. <https://doi.org/10.1080/0013791X.2010.481185>.

Kaiser, M.J., 2012. Profitability assessment of Haynesville shale gas wells. *Energy* 38 (1), 315–330. <https://doi.org/10.1016/j.energy.2011.11.057>.

Kazemi, M., Takbiri-Borujeni, A., 2015. An analytical model for shale gas permeability. *Int. J. Coal Geol.* 146, 188–197. <https://doi.org/10.1016/j.coal.2015.05.010>.

Kazmouz, S.J., Giusti, A., Mastorakos, E., 2016. Numerical simulation of shale gas flow in three-dimensional fractured porous media. *Journal of Unconventional Oil and Gas Resources* 16, 90–112. <https://doi.org/10.1016/j.juogr.2016.10.002>.

Lake, L.W., Baylor, J.M., Ramsey, J.D., Titman, S., 2013. A primer on the economics of shale gas production just how cheap is shale gas? *Bank Am. J. Appl. Corp. Finance* 25 (4), 87–96. <https://doi.org/10.1111/jacf.12041>.

Lebow, D.E., Rudd, J.B., 2003. Measurement error in the consumer price index: where do we stand? *J. Econ. Lit.* 41, 159–201. <https://doi.org/10.1257/002205103321544729>.

León, G., 2012. Comparative analysis of traditional valuation methods applied to the simulation of an investment project. *Business Dimension* 10 (1), 16–21 (in Spanish). URL: <https://dialnet.unirioja.es/servlet/articulo?codigo=4069115>.

Levy, H., Sarnat, M., 1978. Capital Investment and Financial Decisions. Prentice Hall, Washington D.C., USA. <https://doi.org/10.2307/2327195>.

Li, L., Jiang, H., Li, J., Wu, K., Meng, F., Xu, Q., Chen, Z., 2018. An analysis of stochastic discrete fracture networks on shale gas recovery. *J. Petrol. Sci. Eng.* 167, 78–87. <https://doi.org/10.1016/j.petrol.2018.04.007>.

Lindén, J., 2018. Stock price predictions using a geometric Brownian motion. In: *Project Report, Degree Project E in Financial Mathematics*. Uppsala University, Sweden.. URL: <https://www.diva-portal.org/smash/get/diva2:1218088/FULLTEXT01.pdf>.

Liu, H., Zhang, Z., Zhang, T., 2022. Shale gas investment decision-making: green and efficient development under market, technology and environment uncertainties. *Appl. Energy* 306, 118002. <https://doi.org/10.1016/j.apenergy.2021.118002>.

Liu, J., Li, Z., Luo, D., Duan, X., Liu, R., 2020. Shale gas production in China: a regional analysis of subsidies and suggestions for policy. *Util. Pol.* 67, 101135. <https://doi.org/10.1016/j.jup.2020.101135>.

López-Villavicencio, A. and Mignon, V., 2011. On the impact of inflation on output growth: Does the level of inflation matter? *J. Macroecon.* 33 (3), 455–464. <https://doi.org/10.1016/j.jmacro.2011.02.003>.

Malkiel, B.G., 2013. The efficient markets hypothesis and its critics. *J. Econ. Perspect.* 17 (1), 59–82. <https://doi.org/10.1257/089533003321164958>.

Mangiero, G.A., Michael, K., 2017. NPV sensitivity analysis: a dynamic excel approach. *Am. J. Bus. Educ.* 10 (3), 113–126. <https://doi.org/10.19030/ajbe.v10i3.9983>.

- Massey, F.J., 1951. The Kolmogorov-Smirnov test for goodness of fit. *J. Am. Stat. Assoc.* 46 (253), 68–78. <https://doi.org/10.2307/2280095>.
- Mastromatteo, G., Rossi, S., 2015. The economics of deflation in the euro area: a critique of fiscal austerity. *Review of Keynesian Economics* 3 (3), 336–350. <https://doi.org/10.4337/roke.2015.03.04>.
- McKibbin, W.J., Stoeckel, A., 2009. Modelling the global financial crisis. *Oxf. Rev. Econ. Pol.* 25 (4), 581–607. <https://doi.org/10.1093/oxrep/grq012>.
- Melcher, A.J., Melcher, B.H., 1980. Toward a systems theory of policy analysis: static versus dynamic analysis. *Acad. Manag. Rev.* 5 (2), 235–248. <https://doi.org/10.5465/amr.1980.4288738>.
- Mentel, G., Horváthová, Z., 2016. Factors of efficiency of open investment funds in 1997–2015. *Economics & Sociology* 9 (1), 101–114. <https://doi.org/10.14254/2071-789X.2016/9-1/7>.
- Naraghi, M.E., Javadpour, F., 2015. A stochastic permeability model for the shale-gas systems. *Int. J. Coal Geol.* 140, 111–124. <https://doi.org/10.1016/j.coal.2015.02.004>.
- Nassir, M., Settari, A., Wan, R., 2017. Prediction of stimulated reservoir volume and optimization of fracturing in tight gas and shale with a fully elastoplastic coupled geomechanical model. *SPE J.* 19 (5), 771–785. <https://doi.org/10.2118/163814-PA>.
- Nguyen-Le, V., Shin, H., 2019. Development of reservoir economic indicator for Barnett shale gas potential evaluation based on the reservoir and hydraulic fracturing parameters. *J. Nat. Gas Sci. Eng.* 66, 159–167. <https://doi.org/10.1016/j.jngse.2019.03.024>.
- Osborn, S.G., Vengosh, A., Warner, N.R., Jackson, R.B., 2011. Methane contamination of drinking water accompanying gas-well drilling and hydraulic fracturing. *Proc. Natl. Acad. Sci. U. S. A.* 108 (20), 8172–8176. <https://doi.org/10.1073/pnas.1100682108>.
- Papadopoulos, C.E., Yeung, H., 2001. Uncertainty estimation and Monte Carlo simulation method. *Flow Meas. Instrum.* 12 (4), 291–298. [https://doi.org/10.1016/S0955-5986\(01\)00015-2](https://doi.org/10.1016/S0955-5986(01)00015-2).
- Patzek, T.W., Male, F., Marder, M., 2013. Gas production in the Barnett Shale obeys a simple scaling theory. *Proc. Natl. Acad. Sci. U.S.A.* 110 (49), 304–315. <https://doi.org/10.1073/pnas.1313380110>.
- Perez, E., 2014. *Fundamentals of Business Economics*. Ramon Areces Study Center, S.A. Madrid, Spain (in Spanish).
- Poggensee, K., Poggensee, J., 2021. Investment valuation and appraisal: theory and practice. Chapter: *Static Investment Calculation Methods*. Springer, pp. 31–84. URL: <https://books.google.es/>.
- Psarras, P., Holmes, R., Vishal, V., Wilcox, J., 2017. Methane and CO<sub>2</sub> adsorption capacities of kerogen in the Eagle Ford shale from molecular simulation. *Accounts Chem. Res.* 50 (8), 1818–1828. <https://doi.org/10.1021/acs.accounts.7b00003>.
- Rammy, M.H., Awotunde, A.A., 2016. Stochastic optimization of hydraulic fracture and horizontal well parameters in shale gas reservoirs. *J. Nat. Gas Sci. Eng.* 36, 71–78. <https://doi.org/10.1016/j.jngse.2016.10.002>.
- Ranasinghe, M., Russell, A.D., 2006. Analytical approach for economic risk quantification of large engineering projects: validation. *Construct. Manag. Econ.* 10 (1), 45–68. <https://doi.org/10.1080/01446199200000005>.
- Ross, S.A., 1995. Uses, abuses, and alternatives to the Net-Present-Value rule. *Financ. Manag.* 24 (3), 96–102. URL: <https://www.jstor.org/stable/3665561>.
- Sarel, M., 1996. Nonlinear effects of inflation on economic growth. *IMF Econ. Rev.* 43, 199–215. <https://ssrn.com/abstract=883204>.
- Shahsavari, M., Niaki, S.T.A., Najafi, A.A., 2010. An efficient genetic algorithm to maximize net present value of project payments under inflation and bonus–penalty policy in resource investment problem. *Adv. Eng. Software* 41 (7–8), 1023–1030. <https://doi.org/10.1016/j.advengsoft.2010.03.002>.
- Sheather, S.J., Jones, M.C., 1991. A reliable data-based bandwidth selection method for kernel density estimation. *J. Roy. Stat. Soc. B* 53 (3), 683–690. URL: <https://www.jstor.org/stable/2345597>.
- Silin, D., Kneafsey, T., 2012. Shale gas: nanometer-scale observations and well modelling. *J. Can. Pet. Technol.* 464–475. <https://doi.org/10.2118/149489-PA>.
- Soage, A., 2021. *A Numerical Modeling Framework for the Optimization and Economic Analysis of Unconventional Gas Production*. PhD Thesis. University of A Coruna, Coruna, Spain. <https://ruc.udc.es/dspace/handle/2183/28049>.
- Soage, A., Juanes, R., Colominas, I., Cueto-Felgueroso, L., 2024. Optimization of financial indicators in shale-gas wells combining numerical decline curve analysis and economic data analysis. *Energies* 17 (4), 864. <https://doi.org/10.3390/en17040864>.
- Soage, A., Juanes, R., Colominas, I., Cueto-Felgueroso, L., 2021. The impact of the geometry of the effective propped volume on the economic Performance of Shale Gas Well Production. *Energies* 14 (9), 2475. <https://doi.org/10.3390/en14092475>.
- Song, W., Yao, J., Li, Y., Sun, H., Zhang, L., Yang, Y., Sui, H., 2016. Apparent gas permeability in an organic-rich shale reservoir. *Fuel* 181, 973–984. <https://doi.org/10.1016/j.fuel.2016.05.011>.
- Stein, J.C., 1989. Efficient capital markets, inefficient firms: a model of myopic corporate behavior. *Q. J. Econ.* 104 (4), 655–669. <https://doi.org/10.2307/2937861>.
- U.S. Bureau of Labor Statistics, 2022. Consumer Price Index. <https://www.bls.gov/cpi/>.
- Wang, Q., Chen, X., Jha, A.N., Rogers, H., 2014. Natural gas from shale formation – the evolution, evidences and challenges of shale gas revolution in United States. *Renew. Sustain. Energy Rev.* 30, 1–28. <https://doi.org/10.1016/j.rser.2013.08.065>.
- Wang, S., Pomerantz, A.E., Xu, W., Lukyanov, A., Kleinberg, R.L., Wu, Y.S., 2017. The impact of kerogen properties on shale gas production: a reservoir simulation sensitivity analysis. *J. Nat. Gas Sci. Eng.* 48, 13–23. <https://doi.org/10.1016/j.jngse.2017.06.009>.
- Wei, M., Duan, Y., Fang, Q., Zhang, T., 2016. Production decline analysis for a multi-fractured horizontal well considering elliptical reservoir stimulated volumes in shale gas reservoirs. *J. Geophys. Eng.* 13 (3), 354–365. <https://doi.org/10.1088/1742-2132/13/3/354>.
- Weijermars, R., 2013. Economic appraisal of shale gas plays in Continental Europe. *Appl. Energy* 106, 100–115. <https://doi.org/10.1016/j.apenergy.2013.01.025>.
- Wu, Y., Cheng, L., Killough, J.E., Huang, S., Fang, S., Jia, P., Xue, Y., 2021. Integrated characterization of the fracture network in fractured shale gas Reservoirs - stochastic fracture modeling, simulation and assisted history matching. *J. Petrol. Sci. Eng.* 1 (205), 108886. <https://doi.org/10.1016/j.petrol.2021.108886>.
- Yao, J., Sun, H., Fan, D.Y., Wang, C.C., Sun, Z.X., 2013. Numerical simulation of gas transport mechanisms in tight shale gas reservoirs. *Petrol. Sci.* 10, 528–537. <https://doi.org/10.1007/s12182-013-0304-3>.
- Ye, S., Tiong, R.L.K., 2000. NPV-at-risk method in infrastructure project investment evaluation. *J. Construct. Eng. Manag.* 126 (3), 227–233. [https://doi.org/10.1061/\(ASCE\)0733-9364\(2000\)126:3\(227\)](https://doi.org/10.1061/(ASCE)0733-9364(2000)126:3(227)).
- Yu, W., Sepehrnoori, K., Patzek, T., 2016. Modeling gas adsorption in Marcellus shale with Langmuir and BET isotherms. *SPE J.* 21 (2), 589–600. <https://doi.org/10.2118/170801-PA>.
- Yu, W., Sepehrnoori, K., 2013. Optimization of multiple hydraulically fractured horizontal wells in unconventional gas reservoirs. In: *SPE Production and Operations Symposium*, SPE-164509-MS. <https://doi.org/10.2118/164509-MS>. Oklahoma, USA.
- Yuan, J., Luo, D., Feng, L., 2015. A review of the technical and economic evaluation techniques for shale gas development. *Appl. Energy* 148, 49–65. <https://doi.org/10.1016/j.apenergy.2015.03.040>.
- Zhang, C., Shan, W., Wang, X., 2019. Quantitative evaluation of organic porosity and inorganic porosity in shale gas reservoirs using logging data. *Energy Sources, Part A Recovery, Util. Environ. Eff.* 41 (7), 811–828. <https://doi.org/10.1080/15567036.2018.1520361>.
- Zhang, Q., Su, Y., Wang, W., Lu, M., Ren, L., 2017. Performance analysis of fractured wells with elliptical SRV in shale reservoirs. *J. Nat. Gas Sci. Eng.* 45, 380–390. <https://doi.org/10.1016/j.jngse.2017.06.004>.
- Zhao, P., Cai, J., Huang, Z., Ostadhassan, M., Ran, F., 2018. Estimating permeability of shale-gas reservoirs from porosity and rock compositions. *Geophysics* 83 (5), MR283–MR294. <https://doi.org/10.1190/geo2018-0048.1>.
- Zhou, S., Dong, D., Zhang, J., Zou, C., Tian, C., Rui, Y., Jiao, P., 2021. Optimization of key parameters for porosity measurement of shale gas reservoirs. *Nat. Gas. Ind. B* 8 (5), 455–463. <https://doi.org/10.1016/j.ngib.2021.08.004>.